Available online at www.sciencedirect.com
SCIENCE DIRECT
Thin Solid Films 491 (2005) 54 – 60
thin solid films
www.elsevier.com/locate/tsf

Preparation and characterization of high-performance direct current magnetron sputtered ZnO:Al films

W.W. Wang[a,*], X.G. Diao[a], Z. Wang[a], M. Yang[a], T.M. Wang[a], Z. Wu[b]

[a]Center of Material Physics and Chemistry, School of Science, Beihang University, Beijing 100083, China
[b]School of Aeronautic Science and Technology, Beihang University, Beijing 100083, China

Received 15 April 2004; received in revised form 20 October 2004; accepted 13 May 2005
Available online 27 June 2005

Abstract

High-performance aluminium-doped zinc oxide (ZnO:Al) thin films were deposited on glass substrate by direct current reactive magnetron sputtering from a Zn–Al metallic target (Al 3 wt.%). Films with a tangly string-like surface morphology, an average thickness of 837 nm, an optical transmittance up to 85% in the visible range and electrical resistivity down to 1.80×10^{-4} Ω cm were obtained. The dependences of the surface morphology, crystallinity, the electrical and optical properties of the films on substrate temperature, O_2/Ar flow ratio, and sputtering power were investigated using X-ray diffraction, scanning electron microscopy, spectrophotometry, linear array four-point probe, and Hall-effect measurements. The comparison of the surface morphology, crystallinity, and interplanar stress of ZnO:Al films with those of ZnO films was also conducted. The properties are significantly and regularly influenced by the sputtering parameters. The optimal films were prepared with a substrate temperature of 250 °C, O_2/Ar ratio of 10:40 and sputtering power of 55 W. Ionic replacement at the lattice-sites probably induces the decrease of the residual stress and even the reverse of its direction. The correlations between the electrical and the optical characteristics of ZnO:Al films are also discussed in this paper.

PACS: 73.61; 81.15; 78.66
Keywords: ZnO:Al films; Reactive magnetron sputtering; Transparent conductive oxides

1. Introduction

Transparent conductive oxide (TCO) thin films, attributing to their unique and outstanding electrical and optical properties, have attracted much attention and have been used in various optoelectronic devices extensively, such as the transparent electrodes of solar cells and flat panel displays [1,2]. Although In_2O_3:Sn (ITO) thin film, being predominant in the field of application, have successfully met most requirements of TCO films, it has particular disadvantages including toxicity, high price, instability in hydrogen plasma, and degrading active solar cell materials [3]. ZnO:Al thin film, however, is emerging to be a potential and optimal substitute for ITO film due to its cheap and abundant raw materials, non toxicity, and good stability in hydrogen plasma [4]. Furthermore, with high reflectivity to the infrared and its fundamental band gap lying at the end of the luminous spectrum, ZnO:Al thin film shows a potential application for energy-efficient or smart coatings on architectural glasses [5] and heat-reflecting mirrors [6].

Numerous studies on preparation and properties of ZnO:Al films have been conducted using various methods since 1980s [3–7]. Although researchers mainly bend themselves to explore the deposition methods, clarify the influences of the deposition parameters, and obtain first-rank preparation conditions of ZnO:Al films, the actual results are far from the requirement of the perfect properties for practical applications. Therefore, the present research focus still lies in the improvement of the properties of ZnO:Al thin films. Furthermore, fundamental researches such as the effect of grain boundary and

* Corresponding author.
E-mail address: wangww1016@163.com (W.W. Wang).

0040-6090/$ - see front matter © 2005 Elsevier B.V. All rights reserved.
doi:10.1016/j.tsf.2005.05.021

surface morphology, the scattering mechanism, and the structure of energy band, are essential to further investigations on ZnO:Al, ITO thin films and other unborn TCOs.

In this paper, high-performance aluminium-doped zinc oxide thin film with a resistivity of 1.80×10^{-4} Ω cm, a thickness of 837.4 nm, a Hall mobility of 27.4 cm^2/Vs, and an average transmittance of 85% in the visible range is reported. With these outstanding performances, the film possesses a tangly string-like surface morphology observed by scanning electron microscopy (SEM). Moreover, this work indicates the replacement of Zn^{2+} by Al^{3+} through contrasting the X-ray diffraction (XRD) patterns of both ZnO:Al and ZnO thin films. Based on the experiments, the influences of sputtering parameters including substrate temperature (T_s), O_2/Ar flowing ratio, and the sputtering power (P), on significant properties of ZnO:Al films are studied in this paper. Finally, by discussing the correlation between the electrical and optical properties of the films, this study is dedicated to be a groundwork for further investigation and application of ZnO:Al thin films.

2. Experimental details

2.1. Rinsing of the glass substrates

Prior to the deposition of the films, the soda-lime silicon glass substrates (25 mm × 25 mm × 1 mm) were boiled in H_2SO_4 and H_2O_2 solution (volume ratio: 1:3) for 30 min. Afterwards, the substrates were successively rinsed in acetone and ethanol ultrasonic baths for 15 min, respectively. Subsequently, they were rinsed with de-ionized water and dried with N_2 gas. After being fixed on a carrier parallel to the target surface, each substrate was bombarded by Ar^+ for 15 min in the vacuum chamber before the sputtering.

2.2. Preparation and characterization of the ZnO:Al thin films

A direct current (D.C.) magnetron sputtering system was used to deposit ZnO:Al thin film samples. The alloy target of Zn (99.99%)/Al (99.99%) (97:3 wt.%) with a diameter of 60 mm and a thickness of 6 mm was packed and inserted in a water-cooled target holder. The target–substrate distance was 40 mm. Prior to the introduction of sputtering gas, the chamber was evacuated to a pressure lower than 8×10^{-4} Pa by a turbo molecular pump combined with a rotary pump. Sputtering pressure was kept at 1.0 Pa constantly. The flow rates of Ar (99.999%) and O_2 (99.999%) were controlled individually by a couple of mass flow controllers according to the demanded flow ratio. The discharges were generated at an average power in the range of 30–55 W and the substrate temperature was controlled in the 100–300 °C range. After obtaining the required parameters, over 10 min of preliminary sputtering was carried out in order to remove the surface impurity in the target and get into the steady state of sputtering. The deposition time was 15 min for each sample.

The thickness of the films was monitored by an α-step surface profiler (Dektak IIA). X-ray diffraction (XRD) with a Cu Kα source was used to determine the crystalline structure of the samples and the surface morphologies were determined with a Hitachi S-3500 Scanning Electron Microscope using secondary electrons under 25 kV. The transmittance and reflectance spectra were measured using a Lambda 9 Ultraviolet–Visible–Near-infrared spectrophotometer in the spectral range of 300–2600 nm. A linear array four-point probe was used to measure the sheet resistance. Hall measurement was carried out to determine the resistivity, carrier concentration, and Hall mobility of the ZnO:Al thin films. All the characterizations were performed at room temperature.

3. Results and discussion

3.1. Thickness and deposition rate

For 15 min deposition time, the thickness of ZnO:Al thin film samples scatter in the range of 260 nm to 1201 nm. When O_2/Ar flowing ratio was 10:40 and the substrate temperature was 250 °C, the lowest deposition rate 17.3 nm/min appeared at the lowest sputtering power, which was 30 W. As the substrate temperature decreased to 100 °C, the highest deposition rate, 80.0 nm/min, was obtained. Compared with the sputtering power and substrate temperature, the O_2/Ar flowing ratio has little influence on the deposition rate. When T_s and P were respectively kept at 250 °C and 35 W, the average deposition rate changed from 45 nm/min to 35 nm/min as the O_2/Ar flowing ratio increased from 8:42 to 15:35.

To evaluate the uniformity of the thickness, we applied 3 different methods. The first one was observing the color of ZnO:Al thin film samples qualitatively by naked eyes. The surface color of each sample is homogeneous without any interference rings or stripes of different tint, which could indicate the ununiformity of the film thickness. Second, the transmittance spectrum of every sample was measured for three times, with the incident ray aiming at different positions of the ZnO:Al thin film at each time. According to the principle of optical interference, through comparing the distances between the interference peaks of the spectra, the change of film thickness could be deduced. All the spectra of each sample were placed on one graph and were compared with one another. There is no or minor diversity among the interference peak distances for one sample. Quantitative analysis was the third method. Using a α-step surface profiler, three points along the edge (2 cm length) of the step were measured

for each sample. The three results were respectively named d_1, d and d_2. If

$$\Delta d_1 = \sqrt{\left(\frac{d_1 - d}{d}\right)^2} \quad (1)$$

and

$$\Delta d_2 = \sqrt{\left(\frac{d_2 - d}{d}\right)^2}, \quad (2)$$

the uniformity of each thin film sample could be evaluated by the larger of Δd_1 and Δd_2, which was defined as Δd. In this paper, the calculated results of Δd for all samples are in the range of 0.625% to 2.5%, indicating a rather uniform thickness of the sputtered ZnO:Al thin films.

3.2. Structures and surface morphologies

XRD patterns of each ZnO:Al thin film sample were obtained and compared with that of the ZnO thin film sample, which had been prepared using identical sputtering parameters. Fig. 1 shows the typical result of the comparisons. From Fig. 1, three pieces of information could be obtained. Firstly, ZnO:Al films are polycrystalline and highly textured with the *c*-axis perpendicular to the substrate surface just like sputtered ZnO thin films. The strongest peak appearing at 34.3° is attributed to the (002) line of the hexagonal zincite phase, and the other smaller peak at 72.5° represents the (004) diffraction. Secondly, the full width at half maximum (FWHM) of (002) diffraction peak, indicative of the crystallinity of the film and of the size of crystalline grains, decreases with ZnO:Al thin film. Meanwhile, the (002) peak intensity of ZnO:Al thin film sharply increases. Consequently, it seems that Al-doping can improve the crystallinity. Finally, the position of (002) diffraction peak, from which the interplanar distance can be deduced, distinctly moves to a higher value of 2θ when Al is incorporated, which could indicate a decrease of the plane distance in ZnO:Al thin films.

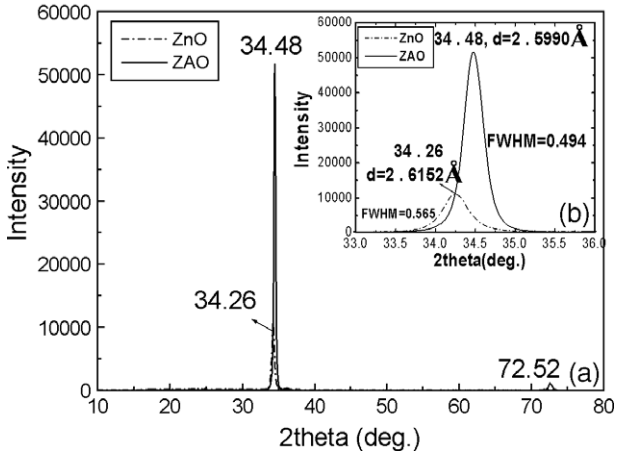

Fig. 1. XRD patterns of ZAO and ZnO films prepared with identical parameters. Substrate temperature was 200 °C. Argon and oxygen fluxes were 40 and 10 sccm, respectively. The sputtering power was 40 W. (a) Original image with 2θ in the range of 10°–80°, (b) magnified image with 2θ in the range of 33°–36°.

It is known that there are interplanar residual stresses parallel to the *c*-axis in sputtered ZnO and ZnO:Al thin films [8,9], because their interplanar distances (d) are different from that of the standard ZnO crystal (2.6000 Å) with the standard location of (002) diffraction peak at 34.45° [10]. Several reports have investigated various methods to reduce the internal stresses of ZnO and ZnO:Al films, including adjusting preparation parameters and annealing after sputtering [8,9,11]. In this work, the interplanar distances of (002) planes of the samples are in the range of 2.5859 Å to 2.6093 Å, while those of the sputtered ZnO thin films are in the range of 2.6049 Å to 2.6437 Å. This result shows that, compared with ZnO thin film, the interplanar residual stress of ZnO:Al thin film decreases and even shifts from tensile stress to compressive stress under certain sputtering conditions. According to the ionic radiuses of Zn^{2+} (0.74 Å) and Al^{3+} (0.54 Å), it could be assumed that the replacement of the former by the latter partly induces the significant alteration of the d-value. Further study and confirmation of this assumption is of great importance because it supplies a rather simple and qualitative method to investigate the doping state of polycrystalline materials possessing interplanar residual stresses.

Fig. 2 shows the surface morphologies of ZnO:Al and ZnO thin films deposited under various conditions. No obvious pinhole defect could be found under the observation of the SEM micrographs. The surface morphology appears to be sensitive to the sputtering parameters since four dissimilar surface morphologies exist in the five samples presented in Fig. 2. The morphology of the ZnO thin film (Fig. 2e) is granular, like most former studies have reported [12]. However, honeycomb morphology (Fig. 2b,d) and the intermediate state (Fig. 2c) between graininess and honeycomb are respectively discovered on different ZnO:Al thin films. It is interesting that Fig. 2a exhibits a morphology bestrewed with a lot of strings tangling together. The "strings" have diameters of 30–80 nm and lengths in the range of 200–1000 nm. The apparent grain sizes observed by SEM are lager than the values deduced from the XRD pattern using Sherrer formula. Similar situations appear in other samples as well (Fig. 2b–e). It seems that the grains demonstrated in SEM micrographs are composed of several small crystal grains especially in Fig. 2a.

Images in Fig. 2 are arranged from (a) to (e) according to the conductivity of the samples they represent. The ZnO:Al thin film sample, owning the morphology showed in Fig. 2a, has the lowest resistivity and the largest Hall mobility of all the samples in this work. Referring to Fig. 2, it can be assumed that, in ZnO:Al thin films, homogeneous and porous morphology induces higher conductivity than the

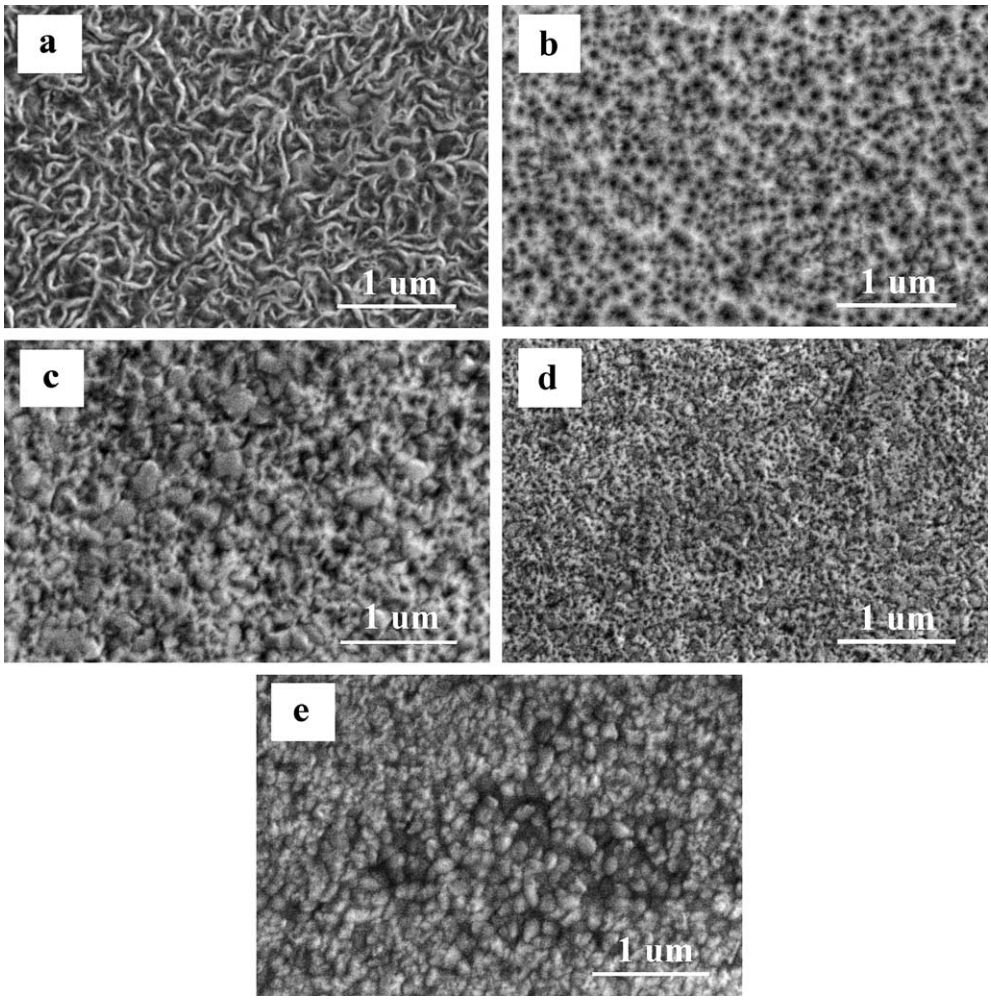

Fig. 2. SEM micrographs of ZnO:Al (except (e)) films prepared with various sputtering parameters. The substrate temperature, O_2/Ar flow ratio and the sputtering power are several: (a) 250 °C, 10:40 and 55 W; (b) 250 °C, 10:40 and 40 W; (c) 150 °C, 10:40 and 40 W; (d) 250 °C, 15:35 and 35 W, respectively. (e) Surface morphology of the ZnO film deposited with a substrate temperature of 200 °C, O_2/Ar ratio of 10:40 and sputtering power of 40 W.

granular one. At the present time, both the attestation of this assumption and the clarification of the correlation between surface morphology and electrical properties demand further experiment and investigation.

3.3. Electrical properties

The dependence of electrical properties on the O_2/Ar flow ratio is shown in Fig. 3. The resistivity of ZnO:Al thin film deposited with a O_2/Ar flow ratio of 5:45 is 3.6 Ω cm, far out of the plotted range in the figure. As the ratio of O_2 increases, the conductivity of ZnO:Al thin films is improved at the beginning then decreased after reaching a top value. The highest carrier concentration and the lowest resistivity are both obtained when the O_2/Ar flow ratio is 8:42 while the top value of Hall mobility appears at 10:40. Subsequently, the resistivity of the ZnO:Al thin film increases gradually from 5.27×10^{-4} Ω cm to 1.88×10^{-2} Ω cm as the O_2/Ar ratio goes on increasing. These results are in accordance with the theoretical explanation by J.M. Huang et al. [13]. When oxygen amount is too low to oxidize all of the sputtered metal atoms, zinc atoms remain un-oxidized and form colloidal zinc because of their less reactivity to oxygen than aluminum atoms. The colloidal Zn seems to be surrounded by the oxidized Al, and accordingly the film shows an extraordinary low conductivity. As oxygen

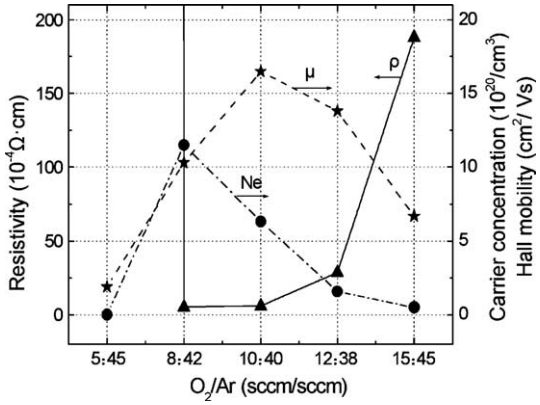

Fig. 3. Dependence of *Ne*, μ, and ρ of ZnO:Al films prepared at substrate temperature of 250 °C and sputtering power of 35 W on O_2/Ar flow ratio.

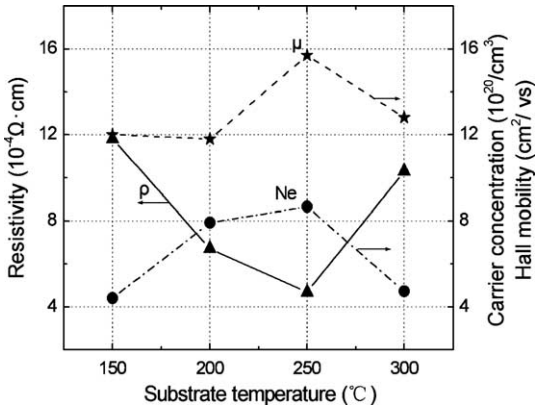

Fig. 4. Dependence of *Ne*, μ, and ρ of ZnO:Al films deposited with a O_2/Ar flow ratio of 10:40 and a sputtering power of 40 W on substrate temperature.

content increases, the hexagonal ZnO is formed and the replacement of Zn^{2+} by Al^{3+} provides conductive electrons, resulting in the improvement of the conductivity. When the O_2/Ar ratio further goes greater, the increase of the resistivity is probably induced by the increase of oxidized aluminium.

Fig. 4 shows the influence of substrate temperature on resistivity (ρ), carrier concentration (*Ne*) and Hall mobility (μ) of ZnO:Al thin films. When the temperature increases from 150 °C to 250 °C, both *Ne* and μ increase. A resistivity of 4.69×10^{-4} Ω cm is obtained at 250 °C. The improvement of the conductivity is caused by the improved crystallinity, decreased amount of interstitial atoms and increased doping of Al^{3+}. However, as the substrate temperature increases further from 250 °C to 300 °C, the situation trends opposite. This conversion can be interpreted by the explanation of X. T. Hao et al. [10]. They reported that high substrate temperature can make some pernicious impurity escape from the substrate, which could abase the crystallinity of the ZnO:Al films.

The sputtering power dependence of ρ, *Ne* and μ of ZnO:Al thin films is shown in Fig. 5. When the sputtering power changes from 30 W to 37.5 W, the resistivity precipitously decreases from 2.02×10^{-2} Ω cm to 5.15×10^{-4} Ω cm. This trend is maintained to 55 W, at which electrical resistivity as low as 1.80×10^{-4} Ω cm is obtained. This low resistivity is caused by a high Hall mobility of 27.4 cm^2/Vs and high carrier concentration of 1.27×10^{21}/cm^3. However, the top value of *Ne* (1.97×10^{21}/cm^3) is achieved at 45 W, although the ρ-value there is higher than 1.80×10^{-4} Ω cm because of the comparatively low Hall mobility (12.8 cm^2/Vs). As the sputtering power grows higher, the increase of μ is mainly due to the

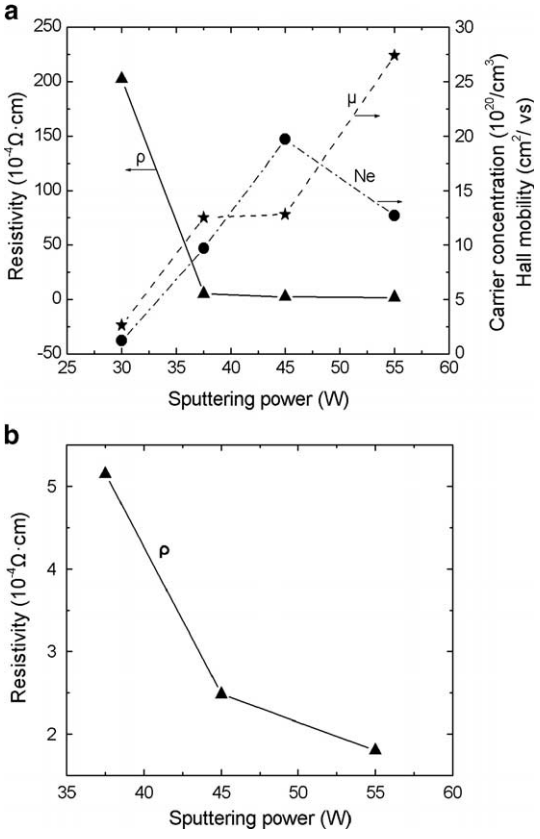

Fig. 5. (a) Influence of sputtering power on *Ne*, μ, and ρ of ZnO:Al films sputtered at substrate temperature of 250 °C and O_2/Ar flow ratio of 10:40. (b) Magnified image to view low ρ-values.

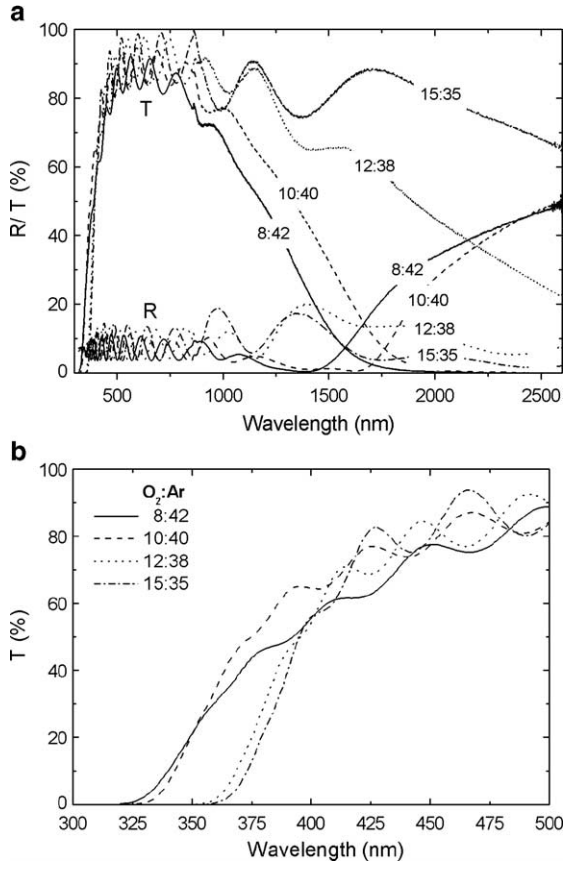

Fig. 6. Transmittance and reflectance spectra of ZnO:Al films deposited with various O_2/Ar flow ratios. Substrate temperature and sputtering power are kept at 250 °C and 35 W, respectively. (a) Integrated spectrum; (b) fundamental absorption.

improvement of crystallinity because the sputtering particles have more sufficient surface diffusion with their energy increased. *Ne* of ZnO:Al thin films is primarily determined by the substitutional doping. According to the assumption about the relationship between Al doping and the d-value mentioned in part 3.1, the ZnO:Al thin film sample deposited at the sputtering power of 45 W should have a lower *d*-value than the film deposited at 55 W does. The actual result is coincident with the assumption with the former *d*-value being 0.0117 Å closer than the latter. Further and detailed investigation is being carried out to determine the influence of sputtering power on the doping stage of ZnO:Al thin films.

3.4. Optical properties

Figs. 6–8 exhibit the optical properties of ZnO:Al thin films prepared with various sputtering parameters. Each sample has a high transmittance to visible light, with an average value over 85%, and a fundamental absorption edge lying in the near-ultraviolet part of the visible spectrum. Obvious interference phenomenon can be observed in every spectrum, indicating a smooth and homogeneous surface of the film. Significant diversities among different samples emerge in near-infrared range and the positions of their absorption edge, as shown in Figs. 6–8.

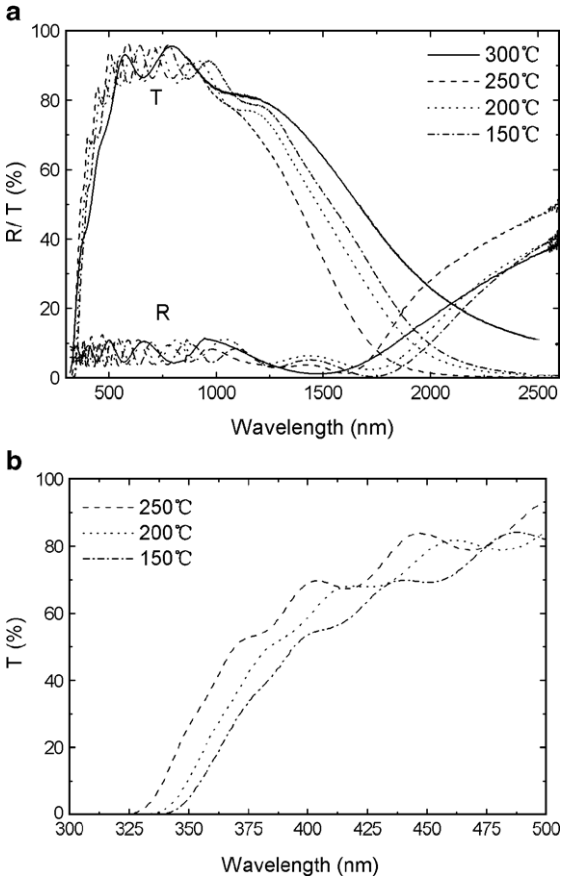

Fig. 7. Transmittance and reflectance spectra of ZnO:Al films deposited at various substrate temperatures. O_2/Ar flow ratio and sputtering power are respectively kept at 10:40 is 40 W. (a) Integrated spectrum; (b) fundamental absorption.

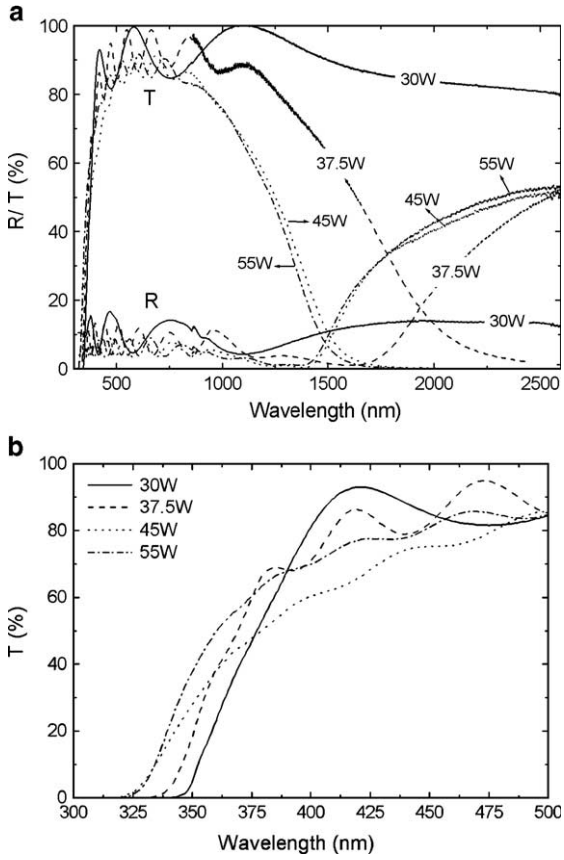

Fig. 8. Transmittance and reflectance spectra of ZnO:Al films deposited with various sputtering power. Substrate temperature is 250 °C and O_2/Ar flow ratio is 10:40. (a) Integrated spectrum; (b) fundamental absorption.

According to the classic Drude theory, there is a correlation between IR reflectance (R) and sheet resistivity (R_s) of thin films, which can be expressed by the following equation [14]

$$R = 1 - \frac{4\varepsilon_0 c_0}{e}\frac{1}{Net\alpha} = 1 - \frac{4\varepsilon_0 c_0}{e}R_s, \quad (3)$$

where ε_0, c_0, e and t represent the permittivity of free space, velocity of light, unit charge , and the thickness of the films respectively. Eq. (3) shows that the IR reflectance will increase linearly when the sheet resistivity decreases. In this paper, the sheet resistivity of ZnO:Al thin films were measured. According to the results of the measurements and the spectra in Figs. 6a 7a 8a, films with a lower R_s have a higher reflectance in near-infrared part., which coincides with Eq. (3). The highest reflectance is owned by ZnO:Al thin film deposited at 55 W (showed in Fig. 8a), whose R_s is as low as 2.15 Ω/□.

The fundamental absorption edge of ZnO:Al thin film can be observed clearly in Figs. 6b 7b 8b. Referring to both the electrical and the optical properties exhibited in this paper, the position of ultraviolet absorption edge is regularly

correlated to the carrier concentration of ZnO:Al thin films. As Ne increases, the position shifts to shorter wavelength, indicating a broadening of the band gap. This is induced by Burstein Moss effect [15], which points out that, in degenerate semiconductor, the increase of Fermi level will lead to a widening of the band gap. In n-type semiconductor, the growth of the band gap is

$$\Delta E_{\mathrm{EM}} = \frac{h^2}{2m_e e}\left(3\pi^2 Ne\right)^{2/3}, \tag{4}$$

where m_e and e is reduced mass and electron charge respectively. The equation shows a $Ne^{2/3}$ dependence of the band gap, which is qualitatively illustrated in this work.

With the unique optical properties, including high IR reflectance, ultraviolet absorption and being transparent to visible light, ZnO:Al thin films have great application potential in smart windows, IR mirrors, and energy-saving materials.

4. Conclusions

High-performance Al-doped zinc oxide thin films were deposited on glass substrates by D.C. reactive magnetron sputtering. Comparing with pure ZnO thin films prepared under the same conditions, the ZnO:Al thin films have an improved crystallinity and decreased, even opposite residual stress. The variations of the residual stress probably indicate the replacement of Zn^{2+} by Al^{3+} during the doping. The substrate temperature, O_2/Ar flow ratio and sputtering power significantly affect the structure, morphology and electrical and optical properties of ZnO:Al thin films. When the above parameters were 250 °C, 10:40 and 55 W, respectively, high-quality aluminium-doped zinc oxide thin film with a resistivity of 1.80×10^{-4} Ω cm, a Hall mobility of 27.4 cm^2/Vs, and an average transmittance over 85% in the visible range was obtained. There are intrinsic correlations between the electrical and optical properties of the ZnO:Al thin films, which are crucial for future study and application of TCO thin films.

Acknowledgements

This work was supported by the National Natural Science Foundation of China (Grant No. 90305026).

References

[1] K. Tabuchi, W.W. Wenas, A. Yamada, M. Konagai, K. Takahashi, Jpn. J. Appl. Phys. 32 (1993) 3764.
[2] C. Beneking, B. Rech, S. Wieder, O. Kluth, H. Wagner, W. Frammelsberger, R. Geyer, P. Lechner, H. Rübel, H. Schade, Thin Solid Films 351 (1999) 241.
[3] K. Ellmer, F. Kudella, R. Mientus, R. Schieck, S. Fiechter, Thin Solid Films 247 (1994) 15.
[4] S. Zafar, C.S. Ferekides, D.L. Morel, J. Vac. Sci. Technol., A 13 (1995) 2177.
[5] G. Granqvist, Appl. Phys., A 57 (1993) 19.
[6] J. Ma, X.T. Hao, S.Y. Zhang, H.L. Ma, J. Mater. Sci. Technol. 19 (2003) 363.
[7] G. Frank, E. Kauer, H. Kostlin, Thin Solid Films 77 (1981) 107.
[8] V. Gupta, A. Mansingh, J. Appl. Phys. 80 (1996) 1063.
[9] M. Chen, Z.L. Pei, C. Sun, L.S. Wen, X. Wang, Mater. Lett. 48 (2001) 194.
[10] X.T. Hao, J. Ma, H.L. Ma, M.H. Tian, B.C. Cao, L.N. Ye, C.F. Cheng, S.Y. Teng, Sci. China, A 45 (2002) 394.
[11] T. Hanabusa, H. Hosoda, K. Kusaka, K. Tominaga, Thin Solid Films 343 (1999) 164.
[12] R.J. Hong, X. Jiang, G. Heide, B. Szyszka, V. Sittinger, W. Werner, J. Cryst. Growth 249 (2003) 461.
[13] J.M. Huang, J.H. Dong, X.Y. Zhang, J. Chongqing Univ. Eng. Ed. 1 (2002) 62.
[14] W.F. Wu, B.S. Chiou, Thin Solid Films 298 (1997) 221.
[15] E. Burstein, Phys. Rev. 93 (1954) 632.